Identification of *N*-benzyl tetrahydroisoquinolines as novel anti-neuroinflammatory agents

Brian Gabet[a], Ping-Chang Kuo[b], Steven Fuentes[a], Yamini Patel[a], Ahmed Adow[a], Mary Alsakka[a], Paula Avila[a], Teri Beam[a], Jui-Hung Yen[b], and Dennis A. Brown[a*]

[a]Manchester University College of Pharmacy and Health Sciences, 10627 Diebold Rd, Fort Wayne, IN 46845

[b]Department of Microbiology and Immunology, Indiana University School of Medicine, 2101 E. Coliseum Blvd, Fort Wayne, IN

*Corresponding author.

Contact information:

Dennis Brown, PhD
Associate Professor – Medicinal Chemistry
Manchester University College of Pharmacy and Health Sciences
10627 Diebold Rd
Fort Wayne, IN 46845
dabrown@manchester.edu

This is the author's manuscript of the article published in final edited form as:

Gabet, B., Kuo, P.-C., Fuentes, S., Patel, Y., Adow, A., Alsakka, M., … Brown, D. A. (2018). Identification of N-benzyltetrahydroisoquinolines as novel anti-neuroinflammatory agents. Bioorganic & Medicinal Chemistry. https://doi.org/10.1016/j.bmc.2018.10.020

Abstract

A series of simplified berberine analogs was designed, synthesized, and evaluated for anti-inflammatory activity. SAR studies identified *N*-benzyl tetrahydroisoquinoline **7d** as a potent berberine analog. **7d** suppressed LPS-induced inflammatory cytokine levels in both BV2 cells and primary microglia. Taken together, our results suggest that simplified BB analogs have therapeutic potential as a novel class of anti-neuroinflammatory agents.

1. Introduction

Multiple sclerosis (MS) is an autoimmune disorder that is characterized by the deterioration of the insulating myelin sheath of neurons in the central nervous system[1]. The interactions of antigen-presenting CNS microglia, CNS infiltrating myelin-specific T cells, and other cells result in the release of pro-inflammatory mediators, ultimately causing brain inflammation leading to myelin deterioration[2]. The symptoms of the disorder are related to the extent of neuronal damage and the location of attack, but can include numbness/weakness in the limbs, vision problems, tremor, slurred speech, electric-shock sensations, fatigue, and bowel and bladder control problems[3].

The importance of inflammation in MS is underscored by the immunomodulatory activity of the current MS therapies. While there are over a dozen disease-modifying MS agents available for the most common type of the disease (relapsing/remitting), there is currently no cure. Additionally, nearly one third of patients develop severe disability. As such, the identification of novel anti-neuroinflammatory agents is warranted.

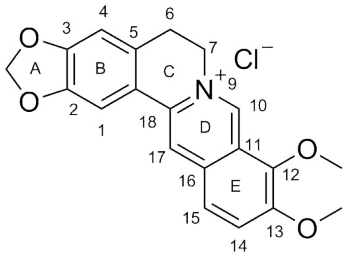

Figure 1. Structure of berberine chloride.

The benzylisoquinolium alkaloid berberine (BB, Figure 1), found in several plant species, has been shown to possess multiple interesting pharmacological properties, including anticancer, antibacterial, antifungal, antidiabetic, and anti-inflammatory activities[4]. Excitingly, BB has been demonstrated to ameliorate inflammatory processes in the experimental autoimmune encephalomyelitis (EAE) model of neuroinflammation[5, 6]. This anti-inflammatory activity has been attributed to modulation of numerous cellular pathways in immune cells, including AMPK, MAPK, Nrf2, and NF-κB[7].

While BB has promising anti-inflammatory activity, it has limited utility as a therapeutic agent. BB suffers from poor solubility, limited absorption, and low bioavailability[8, 9]. Additionally, BB is reported to undergo extensive metabolism with the production of multiple metabolites, some of which are pharmacologically active[10]. The unfavorable pharmacokinetic properties of BB likely are a consequence of several features of its chemical structure: the presence of a contiguous ring system, a permanent positive charge and metabolically-sensitive isoquinolium and alkoxy moieties.

The drug-like properties of BB can likely be improved via structural modification. Numerous structure-activity relationships (SAR) studies have been reported for BB; however, most of

these studies evaluated analogs that are alkylated and/or phenolic derivatives of BB[11-13]. While many of these compounds have displayed interesting activities, most are sufficiently similar to BB to still suffer from poor physicochemical properties. Furthermore, few of these studies explored anti-inflammatory activity. Herein, we report a structure-activity relationships study of simplified BB analogs as anti-neuroinflammatory agents.

2. Chemistry

2.1 Design of initial series of molecules

To probe the structural features of BB that contribute to its anti-inflammatory activity, a series of structurally-diverse molecules was designed (**1-7a**). The roles of the stationary positive charge of the isoquinolium nitrogen, along with the role of planarity on ring D, were evaluated by designing tetrahydroberberine **1** and benzalkonium **2**. The functions of rings C and D were assessed by designing molecules **5-7a**.

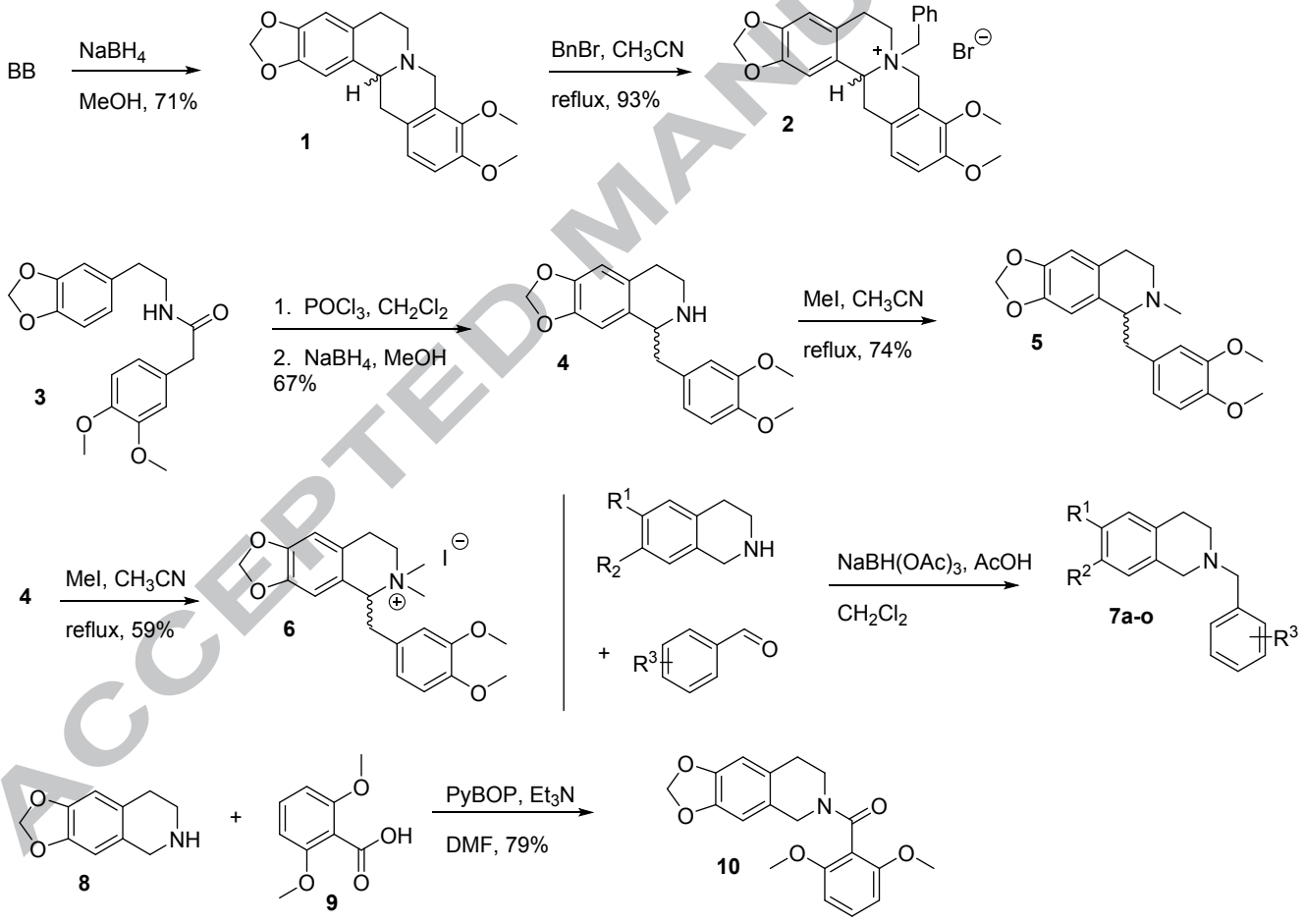

Scheme 1. Synthesis of simplified berberine analogs.

2.2 Synthesis

Compound **1** was prepared as previously described by reducing berberine chloride with $NaBH_4$ in MeOH[14]. Analog **2** was synthesized by treating **1** with benzyl bromide in refluxing CH_3CN[11]. Treatment of amide **3** with first $POCl_3$ followed by $NaBH_4$ provided secondary amine **4**[15]. Methylation of **4** with MeI in refluxing CH_3CN gave amines **5**[16] and **6**. *N*-benzyl analogs **7** were prepared by reductive amination of appropriate benzaldehydes with corresponding tetrahydroisoquinolines using $NaBH(OAc)_3$ in dichloroethane in good yields. Amide **10** was prepared by activating acid **9** with PyBOP with subsequent coupling to amine **8**.

3. Results and discussion

3.1 Evaluation of BB analogs and structure-activity relationship analysis

Tumor necrosis factor (TNF) is one of several important pro-inflammatory cytokines produced by immune cells, including microglia[17]. TNF has been found to be elevated at sites of active MS lesions and contributes to processes that damage oligodendrocytes and myelin[18-20]. Given the importance of TNF in neuroinflammation, synthesized BB analogs were evaluated for their ability to suppress TNF levels induced by lipopolysaccharide (LPS) in the BV2 immortalized mouse microglial cell line. BV2 cells were pretreated with test compounds at a concentration of 50 µM for 1 h, then stimulated with LPS for 24 h, at which time the media was collected and assayed for TNF levels via ELISA. BB was evaluated at a concentration of 1 µM as higher concentrations did not provide additional TNF suppression (data not shown). The results are expressed in Table 1 and are expressed as a percentage of LPS.

As shown in Table 1, treatment of BV2 cells with LPS caused a ten-fold increase of TNF levels. Synthesized molecules demonstrated a range of activities, from significant TNF suppression to minimal. Interestingly, the presence of a permanent cationic nitrogen was as a common feature of the most potent molecules assayed (**BB** and **2**). The nature of the cationic amine appears to be less important, as both isoquinolium (**BB**) and benzalkonium cations (**2**) were tolerated. However, enhanced activity does not seem to apply to cation **6** as minimal TNF suppression was observed (97% of LPS).

Entry	TNF levels (% LPS)
DMSO	10 ± 2.3
LPS	100 ± 0
BB (1 uM)	25 ± 8.2
1	45.0 ± 12
2	22 ± 9.1
4	77 ± 2.4
5	77 ± 5.7
6	97 ± 7.0
7a 1-9 (R^1, R^2 = $-CH_2OCH_2-$), R^3 = 2, 3-OMe	63 ± 8.6

Table 1. Suppression of TNF by synthesized compounds. BV2 cells were treated with DMSO or experimental compounds (50 µM) for 1 hour, followed by LPS (100 ng/mL) activation for 24 hour. The culture media was collected and TNF levels evaluated by ELISA. Data are expressed as mean ± SEM and are representative of three different experiments.

One of our approaches to improve the physicochemical properties of **BB** was to eliminate its permanent positive charge. We were pleased to see that activity can be retained by substitution of the isoquinolium core of BB for tetrahydroisoquinoline (**1**). This molecule suppressed TNF levels to 45% of LPS, suggesting that this portion of the **BB** molecule is amendable to modification.

Ring connectivity also appears to influence TNF suppression. The activity of molecules with the D ring of BB removed appears to depend on the site of C-D ring junction. Compound **7a**, connected to ring D via N9, was more active (63% of LPS) than the analogs **4-6** (77, 77, and 97 % of LPS, respectively), all of which are connected via C18. Indeed, the introduction of an asymmetric center into these compounds may also impact activity.

While **1** and **2** were the most active of the molecules synthesized, their chemical structures still possessed features that were not ideal, namely positive charges and/or a contiguous ring system. *N*-Benzyl tetrahydroisoquinoline **7a**, with its modest activity and synthetic simplicity, seemed a good candidate for optimization. Thus, we designed, synthesized, and evaluated a second series of analogs in an effort to increase TNF-suppression. The results are shown in Table 2.

Entry	R^1	R^2	R^3	TNF levels (% LPS)
DMSO				10 ± 2.3
LPS				100 ± 0
7b	H	H	2, 3-OMe	95 ± 9.4
7c	$-CH_2OCH_2-$		Ph	90 ± 13
7d	$-CH_2OCH_2-$		2, 6-OMe	39 ± 10
7e	$-CH_2OCH_2-$		3, 5-OMe	89 ± 5.2
7f	$-CH_2OCH_2-$		4-OMe	88.± 6.8
7g	$-CH_2OCH_2-$		4-CF_3	102 ± 14
7h	$-CH_2OCH_2-$		2, 4-OMe	103 ± 13
7i	$-CH_2OCH_2-$		2-OMe	78 ± 4.0
7j	$-CH_2OCH_2-$		3-OMe	78 ± 9.6
7k	H	H	2, 6-OMe	78 ± 11
7l	$-CH_2OCH_2-$		2, 6-Me	101 ± 1.3
7m	$-CH_2OCH_2-$		2, 6-Cl	107 ± 6.9
7n	H	OMe	2, 6-OMe	82 ± 5.0
7o	OMe	H	2, 6-OMe	64 ± 9
10				73 ± 11

Table 2. Suppression of TNF by synthesized compounds. BV2 cells were treated with DMSO or experimental compounds (50 μM) for 1 hour, followed by LPS (100 ng/mL) activation for 24 hour. The culture media was collected and TNF levels evaluated by ELISA. Data are expressed as mean ± SEM and are representative of three different experiments.

Compound **7b** lacks the methylenedioxy group of **7a**. This moiety appears to be important for activity as TNF suppression was greatly reduced by its removal (95% of LPS). The substitution of the *N*-benzyl group was next explored by assaying compounds **7c-j**. Excitingly, a substitution

pattern 2, 6-dimethoxy (**7d**) resulted in the most TNF suppression (39% of LPS, compared to 61% for **7a**). In contrast, 2, 4- and 3, 5-dimethoxy substituted analogs **7h** and **7e** gave minimal activity, as did monomethoxy congeners **7f**, **i** and **j**, and trifluoromethyl analog **7g**. *N*-Benzyl analog **7c** also showed minimal activity (89% of LPS).

The introduction of a 2, 6-dimethoxy moiety into compound **7a** clearly augmented its activity; however, it was not clear the extent to which the activity of **7d** could be attributed to this substitution. As such, we synthesized and assayed compounds **7k-o**. Confirming what was observed for **7c**, removal the methylenedioxy of **7d** (**7k**) weakened TNF suppression (79% of LPS). Interestingly, this activity can be partially restored by incorporation of a 6-OMe (**7o**, 64% of LPS), but to a lesser extent than a 7-OMe (**7n**, 82% of LPS) group. The electronic properties of the 2, 6-dimethoxy moiety of **7d** appear to be crucial, as 2, 6-dimethyl (**7l**) or 2, 6-dichloro groups (**7m**) resulted in loss of TNF suppression (101 and 107% of LPS, respectively).

As a cationic nitrogen was seen to give the most activity in **BB** and **1**, it appeared likely that an ionizable nitrogen is needed for **7d**'s activity. This was probed by synthesizing and assaying amide **10**. Expectedly, this molecule was quite weaker than parent **7d** (73 vs. 39% of LPS, respectively). While this decrease in activity is likely due to the loss of ionizability, introduction of conformational restriction may also be involved.

The rationale for the improved activity of **7d** over **7a** is not clear. However, examining low energy conformations of **BB** and **7d** yields a possible explanation (Figure 2). The minimized conformation of **BB** produces an essentially flat structure due to the high degree of sp^2 hybridization in the molecule. The minimized conformation for **7d** suggests that the tetrahydroisoquinoline and *N*-benzyl ring systems are in a perpendicular relationship to each other. Overlaying these two structures shows the methylenedioxy, amine, and 12-methoxy groups of **BB** lining up with their counterparts in **7d**. The other methoxy group of **7d** does not seem to overlap with a group in **BB**. It is possible that this methoxy group is accessing an additional binding site in its target. As the 6 position of the *N*-benzyl ring of **7a** is unsubstituted, this interaction is not possible, and may contribute the weaker activity compared to **7d**.

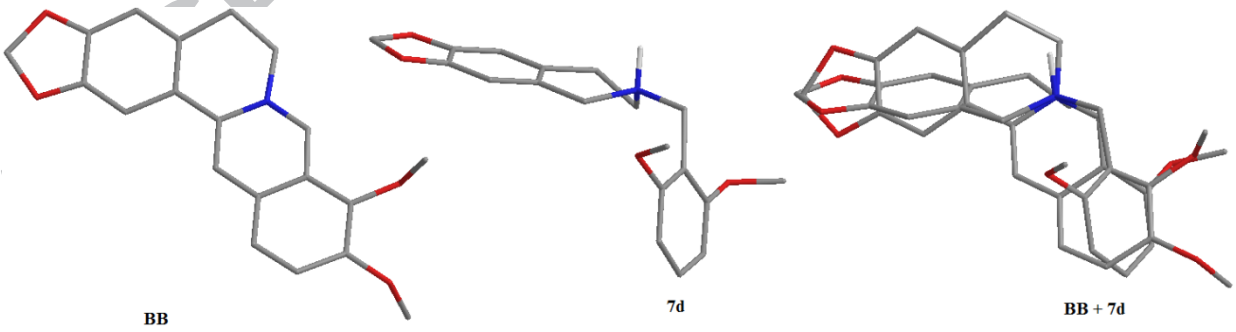

Figure 2. Low energy conformations of BB and 7d using Chem3D.

3.2 Suppression of pro-inflammatory cytokines by 7d

As described above, the production of pro-inflammatory cytokines and mediators are important to the pathophysiology of MS. We next assayed the suppression of these molecules by various concentrations of **7d** in LPS-stimulated BV2 cells. Treatment with LPS alone caused a large increase in TNF release (ten-fold compared to DMSO, Figure 3). Interestingly, treatment with **7d** was able to dose-dependently decrease TNF protein levels was seen beginning at a concentration of 12 μM, and continued to decrease up to 50 μM. IL-6, another pro-inflammatory cytokine, has been demonstrated to be upregulated in both the plasma and CNS of MS patients[21, 22]. As seen for TNF, **7d** was able to suppress LPS-mediated IL-6 induction in a dose-dependent manner, in BV2 cells, beginning at a concentration of at 25 μM.

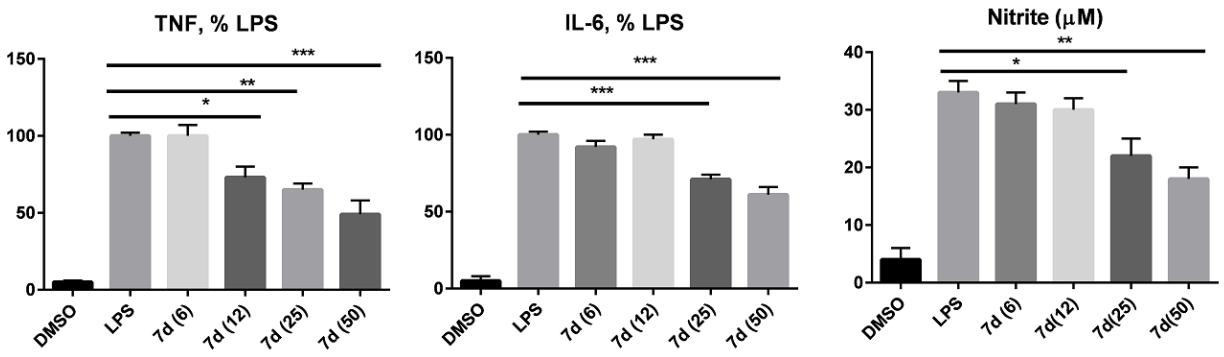

Figure 3. Suppression of TNF, IL-6, and nitrate by **7d**. BV2 cells were treated with **7d** at various concentrations for one hour, followed by LPS (100 ng/mL) for 24 hours. Culture media was then collected and assayed for respective inflammatory products. Data are expressed as mean ± SEM and are representative of three different experiments. Statistical significance determined as * $p < 0.05$, ** $p < 0.01$ and *** $p < 0.001$.

Nitric oxide (NO) is produced by microglia in response to inflammatory stimuli, and is known to contribute to oligodendrocyte injury, demyelination, and axonal degeneration[23]. As NO is converted rapidly to nitrite under physiological conditions, levels of NO_2 were assayed in LPS-stimulated BV2 cells. As seen in Figure 3, LPS treatment induced significant nitrite production. However, treatment with **7d** ameliorated this increase dose-dependently.

The interleukins IL-12, formed from p35 and p40 subunits, and IL-23, formed from p19 and p40 subunits, are important in the development of the pro-inflammatory T_H1 and T_H17 helper T cell phenotypes, respectively[24]. Both of these cell types have are associated with EAE and MS. As such, the mRNA expression of these molecules, along of IL-1β, GM-CSF, TNF, and IL-6 was assessed in LPS-stimulated primary mouse microglia cells. As shown in Figure 4, expression of these genes was increased upon LPS stimulation. Excitingly, however, treatment with **7d** (100 μM) suppressed all but IL-12p40 and TNF, after both 2 and 4 hours of LPS exposure. The suppression of inflammatory cytokines and mediators by **7d** in LPS-stimulated BV2 cells and primary microglia suggest that this compound has anti-neuroinflammatory activity.

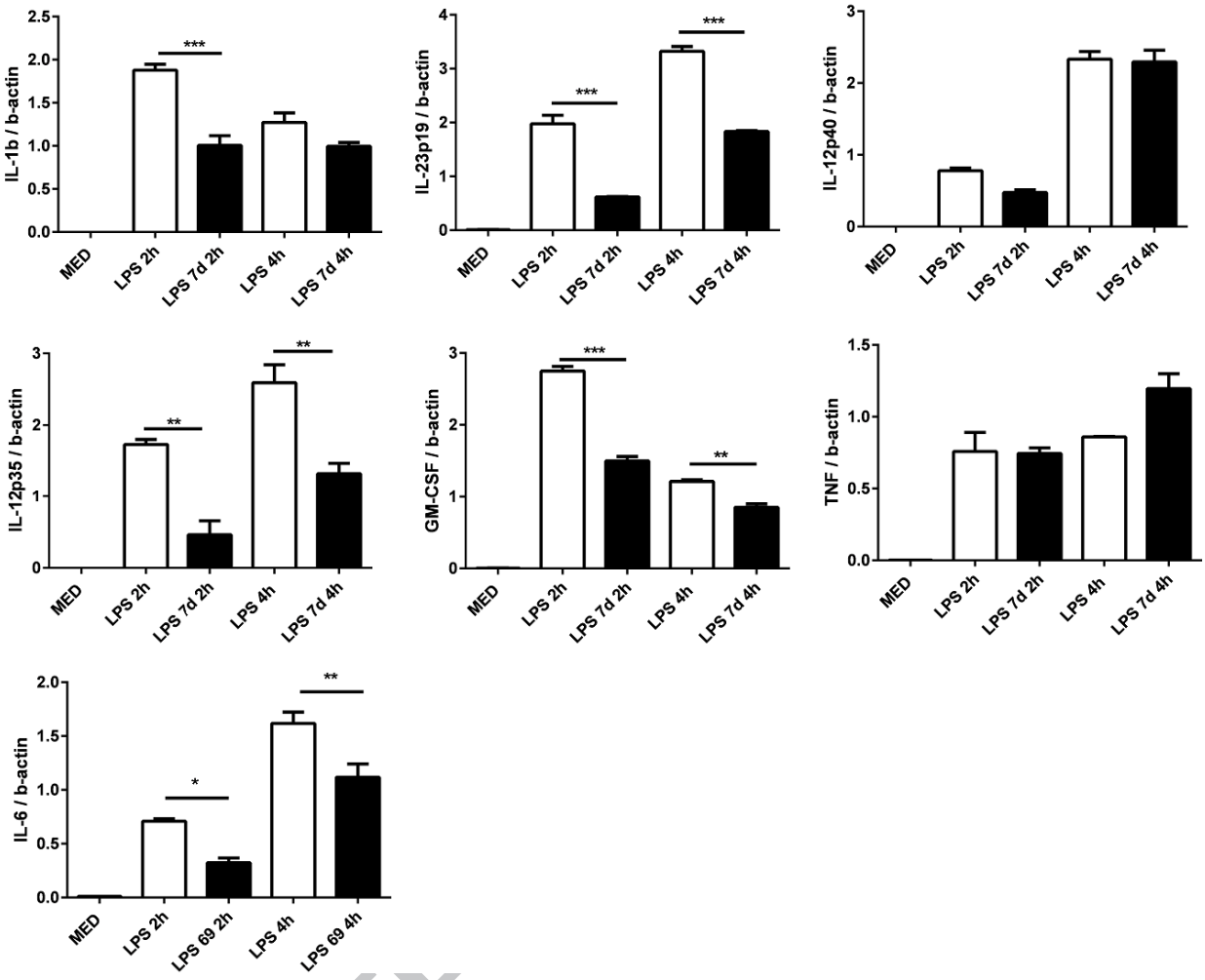

Figure 4. Suppression of inflammatory cytokines by **7d**. Primary microglia cells were treated with **7d** (100 uM) for one hour, followed by stimulation with LPS (100 ng/mL) for 2 and 4 hours. Cells were then harvested and subjected to RNA extraction followed by QPCR analysis of IL-1β, IL-23p19, IL-12p35, IL-12p40GM-CSF, TNF, and IL-6. Data are expressed as mean ± SEM and are representative of three different experiments. Statistical significance determined as * $p < 0.05$, ** $p < 0.01$ and *** $p < 0.001$.

The current unmet medical in need in MS treatment warrants the development of additional therapeutic options. The identification of novel small molecules that target additional inflammatory targets may improve treatment. The anti-inflammatory activity of simplified analog **7d** represents an advancement in the exploration of BB as an immunomodulatory agent. Future planned studies include the determination of mechanism of action of 69, additional structure-activity relationship studies to improve potency, and evaluation the *in vivo* EAE model of neuroinflammation.

4. Conclusion

The isoquinolium alkaloid BB is widely known for its multiple pharmacological activities. However, the therapeutic potential of this interesting natural product is hampered by

unfavorable pharmacokinetic properties arising from aspects of its chemical structure. The results of our studies have delineated the important structural features of BB that influence its anti-inflammatory activity. These studies identified simplified lead compound **7d**, which suppressed LPS-induced inflammatory mediators in both the BV2 cell line and primary microglia, suggesting a potential role for simplified BB analogs as anti-neuroinflammatory agents.

5. Experimental

5.1 Chemistry

All solvents and reagents obtained from commercial sources were used without further purification, unless otherwise noted. Berberine chloride was purchased from TCI (Tokyo, Japan). All reactions were performed under an inert argon atmosphere, unless otherwise indicated. The purity of all final molecules was judged by elemental analyses (C, H, N) and were found to be within ± 0.4% of theoretical values. ^{1}H and ^{13}C NMR analyses were performed on a Varian Mercury 300 spectrophotometer at 300 and 75 MHz, respectively. Chemical shifts are given in ppm in reference to tetramethylsilane (TMS) as an internal standard. Multiplicities are given as s (singlet), d (doublet), t (triplet), m (multiplet), and br s (broad signal). High-resolution mass spectral data were obtained on a Waters Acquity TQD triple quadrupole mass spectrometer. Melting points were taken on a Mel-Temp apparatus and are uncorrected. Thin layer chromatography (TLC) was performed on silica gel 60 F_{254}-coated glass plates purchased from EMD Millipore, and visualized with UV light and/or basic $KMnO_4$. R_f values correspond to the free base, where applicable. Low energy conformations were generated using Chem3D.

General reductive amination procedure. To a solution of tetrahydroisoquinoline (1.41 mmol) and AcOH (2.82 mmol) in $(CH_2Cl)_2$ (5mL) at room temperature was added benzaldehyde (1.41 mmol). The resulting solution was stirred for 15 min, at which time $NaBH(OAc)_3$ (2.82 mmol) was added. The reaction was allowed to proceed overnight, poured into 1 M NaOH (10 mL), and extracted 3 times with CH_2Cl_2. The pooled organic extracts were washed with H_2O, dried over Na_2SO_4, filtered and concentrated. The crude residue was then purified by flash

chromatography (CH_2Cl_2/MeOH). Purified *N*-benzylamines were next converted to their corresponding hydrochloride or oxalate salts.

5-(3,4-dimethoxybenzyl)-6,6-dimethyl-5,6,7,8-tetrahydro-[1,3]dioxolo[4,5-g]isoquinolin-6-ium iodide (6). Tetrahydroisoquinoline **5** (31 mg, 0.095 mmol) and MeI (0.500 mmol) were refluxed in acetonitrile for 4 hours. The reaction mixture was cooled and concentrated. The crude solid was recrystallized from isopropyl alcohol to afford **6** as a white solid (56 mg, 59%). ^{1}H NMR (300 MHz, DMSO-d_6) δ 6.91 – 6.83 (m, 2H), 6.69 (d, *J* = 2.1 Hz, 1H), 6.64 (dd, *J* = 8.2, 2.0 Hz, 1H), 5.97 (d, *J* = 0.9 Hz, 1H), 5.93 (d, *J* = 0.9 Hz, 1H), 5.88 (s, 1H), 4.78 (dd, *J* = 9.4, 4.0 Hz, 1H), 3.81 – 3.54 (m, 8H), 3.32 (s, 4H), 3.11 - 3.08 (m, 5H), 2.89 (dd, *J* = 13.5, 9.4 Hz, 1H). ^{13}C NMR (75 MHz, DMSO) δ 148.6, 147.8, 147.2, 145.2, 128.0, 123.6, 122.7, 122.0, 113.5, 111.7, 108.3, 107.9, 101.2, 71.3, 55.6, 55.5, 53.9, 51.4, 50.4, 36.9, 23.3. HRMS (ESI) *m/z* calcd for: $C_{21}H_{26}NO_4$ M^+ = 356.1862, found: 365.1850.

6-(2,3-dimethoxybenzyl)-5,6,7,8-tetrahydro-[1,3]dioxolo[4,5-g]isoquinoline oxalate (7a). Yield: 77%. White solid (m.p. = 218 – 220 °C). ^{1}H NMR (300 MHz, DMSO-d_6) δ 7.18 – 6.97 (m, 3H), 6.72 (d, *J* = 4.7 Hz, 2H), 5.96 (s, 2H), 4.10 (s, 2H), 3.93 (s, 2H), 3.83 (s, 3H), 3.77 (s, 3H), 3.13 (t, *J* = 6.1 Hz, 2H), 2.87 (t, *J* = 6.1 Hz, 2H). ^{13}C NMR (75 MHz, DMSO) δ 163.4, 152.4, 147.7, 146.4, 145.7, 126.3, 125.5, 124.0, 123.5, 122.9, 113.4, 108.1, 106.4, 100.8, 60.5, 55.7, 53.5, 53.1, 49.1, 26.2. R_f = 0.4 (EtOAc). HRMS (ESI) *m/z* calcd for: $C_{19}H_{21}NO_4$ $[M+H]^+$ = 328.1549, found: 328.1548.

2-(2,3-dimethoxybenzyl)-1,2,3,4-tetrahydroisoquinolineoxalate (7b). Yield: 67%. White solid (m.p. = 167 -169 °C) ^{1}H NMR (300 MHz, DMSO-d_6) δ 9.88 (s, 2H), 7.27 – 7.03 (m, 7H), 4.12 (s, 2H), 4.05 (s, 2H), 3.83 (s, 3H), 3.78 (s, 3H), 3.17 (t, *J* = 6.1 Hz, 2H), 2.98 (t, *J* = 6.1 Hz, 2H). ^{13}C NMR (75 MHz, DMSO) δ 163.4, 152.4, 147.7, 132.4, 130.9, 128.4, 126.9, 126.5, 126.4, 126.1, 124.0, 122.9, 113.4, 60.5, 55.7, 53.7, 53.2, 49.1, 26.3. R_f = 0.5 (EtOAc). HRMS (ESI) *m/z* calcd for: $C_{18}H_{22}NO_2$ $[M+H]^+$ = 284.1651, found: 284.1640.

6-benzyl-5,6,7,8-tetrahydro-[1,3]dioxolo[4,5-g]isoquinoline hydrochloride (7c). Yield: 91%. White solid (m.p. = 235 -238 °C) ^{1}H NMR (300 MHz, DMSO-d_6) δ 11.66 (s, 1H), 7.77 – 7.55 (m, 2H), 7.47 (dp, *J* = 4.8, 1.9 Hz, 3H), 6.77 (d, *J* = 7.1 Hz, 2H), 5.98 (s, 2H), 4.40 (d, *J* = 6.3 Hz, 2H), 4.13 (t, *J* = 4.4 Hz, 2H), 3.55 (s, 1H), 3.20 (d, *J* = 10.8 Hz, 2H), 2.92 (q, *J* = 13.3, 11.4 Hz, 1H). ^{13}C NMR (75 MHz, DMSO) δ 146.8, 146.0, 131.3, 129.8, 129.4, 128.7, 124.8, 120.9, 108.1, 106.3, 101.0, 57.9, 51.0, 48.1, 24.7. R_f = 0.4 (EtOAc). HRMS (ESI) *m/z* calcd for: $C_{17}H_{18}NO_2$ $[M+H]^+$ = 268.1338, found: 268.1324.

6-(2,6-dimethoxybenzyl)-5,6,7,8-tetrahydro-[1,3]dioxolo[4,5-g]isoquinoline oxalate (7d). Yield: 76%. White solid (m.p. = 218 -220 °C) ^{1}H NMR (300 MHz, DMSO-d_6) δ 7.41 (t, *J* = 8.4 Hz, 1H), 6.79 – 6.71 (m, 4H), 5.98 (s, 2H), 4.17 (s, 2H), 4.07 (s, 2H), 3.82 (s, 6H), 3.28 (d, *J* = 6.5 Hz, 2H), 2.92 (t, *J* = 6.3 Hz, 2H). ^{13}C NMR (75 MHz, DMSO) δ 164.1, 159.2, 158.6, 133.1, 131.6, 128.0, 121.6, 113.1, 113.0, 107.0, 104.2, 56.0, 55.2, 52.2, 49.0, 47.4, 25.5. R_f = 0.4 (EtOAc). HRMS (ESI) *m/z* calcd for: $C_{19}H_{22}NO_4$ $[M+H]^+$ = 328.1546, found: 328.1544.

6-(3,5-dimethoxybenzyl)-5,6,7,8-tetrahydro-[1,3]dioxolo[4,5-g]isoquinoline oxalate (7e). Yield: 81%. White solid (m.p. = 219 -221°C) ^{1}H NMR (300 MHz, DMSO-d_6) δ 6.74 (d, *J* = 4.5 Hz, 2H), 6.67 (d, *J* = 2.3 Hz, 2H), 6.52 (t, *J* = 2.2 Hz, 1H), 5.97 (s, 2H), 4.07 (s, 2H), 3.93 (s, 2H), 3.75 (s, 6H), 3.14 (t, *J* = 6.2 Hz, 2H), 2.89 (t, *J* = 6.1 Hz, 2H). ^{13}C NMR (75 MHz, DMSO) δ 164.1, 161.0, 146.9, 146.3, 126.0, 123.7, 108.6, 108.4, 107.0, 101.3, 100.8, 59.8, 55.7, 53.3, 49.4, 26.5. R_f = 0.3 (EtOAc). HRMS (ESI) *m/z* calcd for: $C_{19}H_{22}NO_4$ $[M+H]^+$ = 328.1546, found: 328.1545.

6-(4-methoxybenzyl)-5,6,7,8-tetrahydro-[1,3]dioxolo[4,5-g]isoquinoline hydrochloride (7f). Yield: 94%. White solid (m.p. = 231 -233°C) ^{1}H NMR (300 MHz, DMSO-d_6) δ 11.48 (s, 1H), 7.63 – 7.55 (m, 2H), 7.07 – 6.95 (m, 2H), 6.77 (d, *J* = 5.8 Hz, 2H), 5.98 (s, 2H), 4.43 – 4.24 (m, 2H), 4.10 (d, *J* = 5.4 Hz, 2H), 3.79 (s, 3H), 3.54 (d, *J* = 4.3 Hz, 1H), 3.23 – 3.12 (m, 2H), 2.97 – 2.82 (m, 1H). ^{13}C NMR (75 MHz, DMSO) δ 160.0, 146.8, 146.0, 132.8, 124.8, 121.5, 121.0, 114.1, 108.1, 106.3, 101.0, 57.5, 55.2, 50.8, 47.9, 24.7. R_f = 0.4 (EtOAc). HRMS (ESI) *m/z* calcd for: $C_{18}H_{20}NO_3$ $[M+H]^+$ = 298.1443, found: 298.1435.

6-(4-(trifluoromethyl)benzyl)-5,6,7,8-tetrahydro-[1,3]dioxolo[4,5-g]isoquinoline oxalate (7g). Yield: 67%. White solid (m.p. = 219 -222 °C) ^{1}H NMR (300 MHz, DMSO-d_6) δ 7.83 – 7.64 (m, 4H), 6.72 (s, 1H), 6.68 (s, 1H), 5.95 (s, 2H), 4.12 (s, 2H), 3.82 (s, 2H), 3.04 (t, *J* = 6.0 Hz, 2H), 2.85 (t, *J* = 6.1 Hz, 2H). ^{13}C NMR (75 MHz, DMSO) δ 163.0, 146.2, 145.6, 139.1, 130.6, 128.9, 128.5, 125.8, 125.4, 125.3, 124.2, 108.1, 106.3, 100.7, 59.1, 53.4, 49.4, 26.7. R_f = 0.4 (EtOAc). HRMS (ESI) *m/z* calcd for: $C_{18}H_{17}FNO_2$ $[M+H]^+$ = 336.1200, found: 336.1203.

6-(2,4-dimethoxybenzyl)-5,6,7,8-tetrahydro-[1,3]dioxolo[4,5-g]isoquinoline oxalate (7h). Yield: 70%. White solid (m.p. = 187 -189 °C) ^{1}H NMR (300 MHz, DMSO-d_6) δ 7.36 (d, *J* = 8.4 Hz, 1H), 6.75 (d, *J* = 4.8 Hz, 2H), 6.64 (d, *J* = 2.4 Hz, 1H), 6.59 (dd, *J* = 8.4, 2.4 Hz, 1H), 5.98 (s, 2H), 4.10 (s, 2H), 4.00 (s, 2H), 3.82 (s, 3H), 3.80 (s, 3H), 3.20 (t, *J* = 6.3 Hz, 2H), 2.90 (t, *J* = 6.3 Hz, 2H). ^{13}C NMR (75 MHz, DMSO) δ 163.1, 161.4, 159.2, 146.5, 145.9, 132.7, 125.6, 123.4, 112.8, 108.1, 106.4, 105.4, 100.8, 98.7, 55.7, 55.4, 53.4, 52.8, 48.8, 26.1. R_f = 0.3 (EtOAc). HRMS (ESI) *m/z* calcd for: $C_{19}H_{22}NO_4$ $[M+H]^+$ = 328.1540, found: 328.1542.

6-(2-methoxybenzyl)-5,6,7,8-tetrahydro-[1,3]dioxolo[4,5-g]isoquinoline oxalate (7i). Yield: 78%. White solid (m.p. = 208 - 210 °C^{1}H NMR (300 MHz, DMSO-d_6) δ 7.54 – 7.32 (m, 2H), 7.20 – 7.07 (m, 1H), 7.00 (t, *J* = 7.3 Hz, 1H), 6.74 (d, *J* = 7.0 Hz, 2H), 5.97 (s, 1H), 4.12 (s, 1H), 3.97 (s, 1H), 3.83 (s, 1H), 3.17 (s, 1H), 2.90 (d, *J* = 6.0 Hz, 1H). ^{13}C NMR (75 MHz, DMSO) δ 163.9, 157.9, 146.5, 145.8, 132.1, 130.6, 125.2, 122.8, 120.4, 111.2, 108.1, 106.4, 100.9, 55.5, 53.1, 52.5, 48.8, 25.6. R_f = 0.5 (EtOAc). HRMS (ESI) *m/z* calcd for: $C_{18}H_{20}NO_3$ $[M+H]^+$ = 298.1443, found: 298.1436.

6-(3-methoxybenzyl)-5,6,7,8-tetrahydro-[1,3]dioxolo[4,5-g]isoquinoline oxalate (7j). Yield: 83%. White solid (m.p. = 235 -238 °C). ^{1}H NMR (300 MHz, DMSO-d_6) δ 7.33 (t, *J* = 7.8 Hz, 1H), 7.09 – 6.89 (m, 3H), 6.72 (d, *J* = 7.9 Hz, 2H), 5.95 (s, 2H), 4.04 (d, *J* = 10.6 Hz, 2H), 3.91 – 3.81 (m, 2H), 3.76 (s, 3H), 3.08 (d, *J* = 8.7 Hz, 2H), 2.87 (d, *J* = 6.5 Hz, 2H). ^{13}C NMR (75 MHz, DMSO) δ 162.9, 159.7, 146.5, 145.9, 135.7, 129.7, 126.1, 124.4, 122.2, 115.5, 114.2, 108.2, 106.5, 100.8,

60.0, 55.3, 53.6, 49.7, 26.7. R_f = 0.4 (EtOAc). HRMS (ESI) *m/z* calcd for: $C_{18}H_{20}NO_3$ $[M+H]^+$ = 298.1443, found: 298.1440.

2-(2,6-dimethoxybenzyl)-1,2,3,4-tetrahydroisoquinoline oxalate (7k). Yield: 96%. White solid (m.p. = 193 -195 ^oC). ^1H NMR (300 MHz, DMSO-d_6) δ 7.41 (t, *J* = 8.4 Hz, 1H), 7.31 – 7.11 (m, 4H), 6.75 (d, *J* = 8.4 Hz, 2H), 4.19 (s, 4H), 3.82 (s, 6H), 3.39 – 3.28 (m, 2H), 3.03 (t, *J* = 6.4 Hz, 2H). ^{13}C NMR (75 MHz, DMSO) δ 163.3, 159.2, 132.1, 131.1, 130.3, 128.3, 127.1, 126.6, 126.1, 108.1, 104.3, 56.0, 52.9, 49.2, 47.7, 39.8, 25.6. R_f = 0.5 (EtOAc). HRMS (ESI) *m/z* calcd for : $C_{18}H_{22}NO_2$ $[M+H]^+$ = 284.1651, found: 284.1642.

6-(2,6-dimethylbenzyl)-5,6,7,8-tetrahydro-[1,3]dioxolo[4,5-g]isoquinoline oxalate (7l). Yield: 63%. White solid (m.p. = 196 -198 $^oC$$^1H$ NMR (300 MHz, DMSO-d_6) δ 7.33 – 6.93 (m, 3H), 6.68 (s, 2H), 5.93 (s, 2H), 3.86 (s, 2H), 3.81 – 3.63 (m, 2H), 2.92 (s, 2H), 2.75 (t, *J* = 6.0 Hz, 2H), 2.37 (s, 6H). ^{13}C NMR (75 MHz, DMSO) δ 161.9, 146.1, 145.7, 138.2, 132.8, 128.3, 127.6, 126.6, 126.2, 108.2, 106.4, 100.6, 54.7, 54.6, 49.8, 27.9, 19.9. R_f = 0.4 (EtOAc). HRMS (ESI) *m/z* calcd for: $C_{19}H_{22}NO_2$ $[M+H]^+$ = 296.1651, found: 296.1645.

6-(2,6-dichlorobenzyl)-5,6,7,8-tetrahydro-[1,3]dioxolo[4,5-g]isoquinoline oxalate (7m). Yield: 67%. White solid (m.p. = 153 - 157 ^oC) ^1H NMR (300 MHz, DMSO-d_6) δ 7.55 – 7.46 (m, 2H), 7.38 (dd, *J* = 8.9, 7.1 Hz, 1H), 6.63 (d, *J* = 4.2 Hz, 2H), 5.92 (s, 2H), 3.94 (s, 2H), 3.68 (s, 2H), 2.85 (t, *J* = 5.9 Hz, 2H), 2.70 (t, *J* = 5.9 Hz, 2H). ^{13}C NMR (75 MHz, DMSO) δ 161.3, 145.8, 145.4, 136.2, 130.3, 128.7, 126.4, 108.1, 106.3, 100.5, 55.3, 54.9, 50.1. R_f = 0.4 (EtOAc). HRMS (ESI) *m/z* calcd for: $C_{17}H_{16}NO_2Cl_2$ $[M+H]^+$ = 336.0559, found: 336.0558.

2-(2,6-dimethoxybenzyl)-7-methoxy-1,2,3,4-tetrahydroisoquinoline oxalate (7n). Yield: 69%. White solid (m.p. = 180 -181 $^oC$$^1H$ NMR (300 MHz, DMSO-d_6) δ 7.41 (t, *J* = 8.4 Hz, 1H), 7.12 (d, *J* = 8.4 Hz, 1H), 6.84 (dd, *J* = 8.4, 2.7 Hz, 1H), 6.80 – 6.68 (m, 3H), 4.17 (d, *J* = 15.0 Hz, 4H), 3.82 (s, 6H), 3.73 (s, 3H), 3.33 (s, 2H), 2.95 (t, *J* = 6.4 Hz, 2H). ^{13}C NMR (75 MHz, DMSO) δ 164.1, 159.1,

157.7, 131.5, 130.6, 129.5, 123.5, 114.0, 111.2, 106.7, 104.0, 55.9, 55.2, 52.4, 49.2, 47.2, 24.3. R_f = 0.5 (EtOAc). HRMS (ESI) *m/z* calcd for: $C_{19}H_{24}NO_3$ $[M+H]^+$ = 314.1756, found: 314.1764.

2-(2,6-dimethoxybenzyl)-6-methoxy-1,2,3,4-tetrahydroisoquinoline oxalate (7o). Yield: 55%. White solid (m.p. = 186 – 188 °C) ^{1}H NMR (300 MHz, DMSO-d_6) δ 7.41 (t, *J* = 8.4 Hz, 1H), 7.10 (d, *J* = 8.4 Hz, 1H), 6.87 – 6.57 (m, 4H), 4.19 (s, 2H), 4.13 (s, 2H), 3.82 (s, 6H), 3.74 (s, 3H), 3.44 – 3.22 (m, 2H), 3.02 (t, *J* = 6.4 Hz, 2H). ^{13}C NMR (75 MHz, DMSO) δ 164.1, 159.2, 158.6, 133.1, 131.6, 128.0, 121.6, 113.1, 113.0, 107.0, 104.2, 56.0, 55.2, 52.2, 49.0, 47.4, 25.5. R_f = 0.5 (EtOAc). HRMS (ESI) *m/z* calcd for: $C_{19}H_{24}NO_3$ $[M+H]^+$ = 314.1756, found: 314.1751.

(7,8-dihydro-[1,3]dioxolo[4,5-g]isoquinolin-6(5H)-yl)(2,6-dimethoxyphenyl)methanone (10). To a solution of 2,6-dimethoxybenzoic acid (150 mg, 0.824 mmol) in DMF (3 mL) was added sequentially trimethylamine (2.74 mmol) and PyBOP (514 mg, 1.00 mmol). The solution was stirred at ambient temperature for 10 minutes. Next, 5,6,7,8-tetrahydro-[1,3]dioxolo[4,5-g]isoquinoline (146 mg, 0.824 mmol) was added and the reaction was allowed to proceed for a further 3 hours, at which time the solution was poured into water (50 mL) and extracted three times with Et_2O (50 mL). The pooled organic extracts were washed with H_2O, dried over Na_2SO_4, filtered and concentrated. The crude residue was then purified by flash chromatography (EtOAc) to yield the titled compound (221 mg, 79%). White solid (m.p. = 161 – 164 °C). NMR analysis showed the presence of two rotamers in a ratio of 2:1, which was confirmed by temperature-resolved NMR experiments (see Supporting Information). ^{1}H NMR Major rotamer: (300 MHz, DMSO-d_6) δ 7.34 (t, *J* = 8.4 Hz, 1H), 6.82 (s, 1H), 6.78 – 6.64 (m, 3H), 5.96 (s, 2H), 4.65 (s, 2H), 3.73 (s, 6H), 3.30 (dd, *J* = 6.3, 5.4 Hz, 2H), 2.61 (t, *J* = 5.8 Hz, 2H). ^{1}H NMR Minor rotamer: (300 MHz, DMSO-d_6) δ 7.33 (t, *J* = 8.4 Hz, 1H), 6.75 - 6.69 (m, 3H), 6.58 (s, 1H), 5.93 (s, 2H), 4.17 (s, 2H), 3.75 (t, *J* = 5.8 Hz, 2H), 3.63 (s, 6H), 2.73 (t, *J* = 5.8 Hz, 2H). ^{13}C NMR Combined rotamers (101 MHz, DMSO) δ 164.7, 156.7, 156.6, 146.3, 146.2, 146.1, 146.1, 130.8, 130.7, 128.1, 127.8, 126.9, 126.5, 115.0, 114.8, 108.9, 108.8, 107.0, 106.4, 104.8, 104.7, 101.1, 101.0, 56.2, 47.8, 43.9, 43.7, 29.3, 28.4. HRMS (ESI) *m/z* calcd for: $C_{19}H_{19}NO_5$ $[M+H]^+$ = 342.1341, found: 342.1335.

5.2 Pharmacology

5.2.1 Cell culture conditions

The BV2 microglial cell line a generous gift from Dr. Yen (Fort Wayne, IN). Cells were grown in DMEM:F-12 media (1:1) supplemented with 10% heat-inactivated FBS and 100 U/mL penicillin and 100 µg/mL streptomycin in 150 cm^2 culture flasks in a humidified atmosphere of 5% CO_2. The media was replaced every 2 days, and cells were subcultured once a confluence of 70-80% was reached. All test compounds were dissolved in DMSO and diluted in media (final DMSO concentration of 0.1% v/v).

Primary MG were generated as previously described.[25] Briefly, cerebral cortical cells from 1-2 days old neonatal mice were plated in 75-cm^2 culture flasks DMEM/F12 (1:1) supplemented with 10% heat-inactivated FBS, containing 2mM glutamine and 1X antibiotic/antimycotic (complete medium). After days 3 and 6 of plating, the medium was removed and replaced with fresh complete medium containing 5 ng/ml GM-CSF. MG were then harvested at day 13 or 14 by shaking the flasks at 350 rpm for 30 min at 37°C. Collected cells were subsequently plated for use.

5.2.2 Cytokine quantification assay

BV2 cells were plated in 12 well plates at a density of 5 x 10^5 cells/mL and allowed to attach overnight. Cells were then treated with either DMSO or test compounds for one hour, followed by LPS (*E. coli* O55:B5, 100 ng/mL, Sigma) treatment for 24 hours. Media was then collected, centrifuged to remove floating cells, and either assayed immediately or frozen at -80 ^oC for future use. TNF or IL-6 levels were determined using Ready Set Go! ELISA kit from Thermofisher.

5.2.3 Nitrate quantification assay

BV2 cells were plated in 12 well plates at a density of 5 x 10^5 cells/mL and allowed to attach overnight. Cells were then treated with either DMSO or test compounds for one hour, followed by LPS treatment for 24 hours. Media was then collected, centrifuged to remove floating cells, and either assayed immediately or frozen at -80 ^oC for future use. Media samples were assayed for nitrite levels using the Greis assay kit from Thermofisher.

5.2.4 QPCR analysis

After collection primary MG were plated (5 x 10^5 cells/mL) and allowed to attach overnight. Cells were then treated with either DMSO or test compound for one hour, followed by LPS (100 ng/mL) for 2 and 4 hours. Following treatment, primary MG were subjected to RNA extraction, purification, and quantification using the Trizol reagent (Thermofisher), followed by cDNA synthesis using the High Capacity Reverse Transcription cDNA kit (Thermofisher). Expression of Il-1β, Il-12p35, Il-12p40, Il-23p19, GM-CSF, TNF, and Il-6 were detected by quantitative PCR as previous described.[26] The primers used were Il-1β: sense 5'-CCCTGCAGCTGGAGAGTGTGGA-3' and antisense 5'-TGTGCTCTGCTTGGAGGTGCTG-3'; Il-12p35: sense 5'-CTGTGCCTTGGTAGCATCTATG -3' and anti-sense 5'-GCAGAGTCTCGCCATTATGATTC-3'; Il-12p40: sense 5'-TGGTTTGCCATCGTTTTGCTG-3' and antisense 5'-ACAGGTGAGGTTCACTGTTTCT-3'; Il-23p19: sense 5'-TGCTG GATTGCAGAGCAGTAA-3' and anti-sense 5'-GCATGCAGAGATTCCGAGAGA-3'; GM-CSF: sense 5'-ATGCCTGTCACGTTGAATGAAG-3' and anti-sense 5'-GCGGGTCT GCACACATGTTA-3'; TNF: sense 5'-ATGGCCTCCCT-CTCATCA-GT-3' and antisense 5'-CTTGGTGGTTTGCTACGACG-3'; IL-6: sense 5'-TCCTCTCTGCAAGAGACTTCCATCC-3' and antisense 5'-GGGAAGG-CCGTGGTTGTCACC-3'.

6. Statistical analysis

Results are expressed as mean ± SEM. Comparisons among multiple groups were done by one-way ANOVA, followed by Dunnett's *post hoc* test. Statistical significance was determined as p values ≤ 0.05. GraphPad Prism 5 was used to perform all analyses.

Funding

This work was funded by the Manchester University Pharmacy Programs Internal Research Grant to DB and by the Anna Yoder Multiple Sclerosis Fund to JY.

Declarations of interest

The authors declare there are no conflicts of interest.

Abbreviations.

BB: berberine
CNS: central nervous system
EAE: experimental autoimmune encephalomyelitis
LPS: lipopolysaccharide
MS: multiple sclerosis

Keywords. Berberine, neuroinflammation, multiple sclerosis

References

1. Compston A, Coles A. *The Lancet*.372:1502-1517.
2. Brück W, Porada P, Poser S, et al. *Ann. Neurol.* 1995;38:788-796.
3. Symptoms and Diagnosis. http://www.nationalmssociety.org/Symptoms-Diagnosis. (2017).
4. Imenshahidi M, Hosseinzadeh H. *Phytother. Res.* 2016;30:1745-1764.
5. Luo J, Chen R, Zeng S, et al. *Biochem. Biophys. Res. Commun.* 2017;490:927-932.
6. Jiang Y, Wu A, Zhu C, et al. *Neurol. Res.* 2013;35:360-368.
7. Li Z, Geng Y-N, Jiang J-D, et al. *J. Evid. Based. Complementary Altern. Med*. 2014;2014:12.
8. Battu SK, Repka MA, Maddineni S, et al. *AAPS PharmSciTech*. 2010;11:1466-1475.
9. Godugu C, Patel AR, Doddapaneni R, et al. *PLoS One*. 2014;9:e89919.
10. Wang K, Feng X, Chai L, et al. *Drug. Metab. Rev.* 2017;49:139-157.
11. Li Y-H, Yang P, Kong W-J, et al. *J. Med. Chem.* 2009;52:492-501.
12. Jin X, Yan T-H, Yan L, et al. *Drug Des. Devel. Ther*. 2014;8:1047-1059.
13. Zhang S, Wang X, Yin W, et al. *Bioorg. Med. Chem. Lett.* 2016;26:4799-4803.
14. Nechepurenko I, Boyarskikh U, Khvostov M, et al. *Chem. Nat. Compd.* 2015;51:916-922.
15. Huang WJ, Singh OV, Chen CH, et al. *Helv. Chim. Acta*. 2004;87:167-174.
16. Stenlake John BStenlake JB. *Eur. J. Med. Chem*. 1981;16:515-524.
17. Kollias G, Douni E, Kassiotis G, et al. *Immunol. Rev.* 1999;169:175-194.
18. Selmaj K, Raine CS, Cannella B, et al. *J. Clin. Invest.* 1991;87:949-954.
19. Selmaj KWRaine CS. *Ann. Neurol.* 1988;23:339-346.
20. Selmaj K, Raine CS, Farooq M, et al. *J. Immunol.* 1991;147:1522-1529.
21. Krei K, Fredrikson S, Fontana A, et al. *J. Neuroimmunol.* 1991;31:147-153.
22. Maimone D, Guazzi GC, Annunziata P. *J. Neurol. Sci.* 1997;146:59-65.
23. Smith KJ, Lassmann H. *Lancet Neurol*. 2002;1:232-241.
24. Fletcher JM, Lalor SJ, Sweeney CM, et al. *Clin. Exp. Immunol.* 2010;162:1-11.
25. Kuo P-C, Yu IC, Scofield BA, et al. *Brain, Behav., Immun.* 2017;62:180-192.
26. Kuo PC, Scofield BA, Yu IC, et al. *J. Am. Heart Assoc*. 2016;5:e002610.